<u>Investigations</u>

Historical Climate Change Dynamics Facilitated Speciation and Hybridization Between Highland and Lowland Species of *Baripus* Ground Beetles From Patagonia

Melisa Olave[1,2,3] , Mariana Griotti[1] , Roldolfo Carrara[1] , Paolo Franchini[3] , Axel Meyer[3] , Sergio A. Roig-Juñent[1,2,4]

[1] Argentine Dryland Research Institute of the National Scientific and Technical Research Council (IADIZA-CONICET), [2] Exact and Natural Sciences, National University of Cuyo, [3] Department of Biology, University of Konstanz, [4] Animal Biology Institute, Agricultural Sciences, National University of Cuyo

Bulletin of the Society of Systematic Biology

Abstract

One of the largest beetles of Patagonia, *Baripus* (*Cardiophthalmus*), includes 20 currently described species. Its distribution ranges from the tip of Patagonia, on Tierra del Fuego Island, to isolated patches along the Andes and extra-Andes mountains in northern Patagonia on the Payunia at >3000 m elevation. Here, using RADseq data, evidence is found of mixed ancestry in different lineages. Phylogenetic network reconstruction shows two hybridizing edges between lowland and highland species. Using environmental niche modeling, we show changes in geographic distribution of potential niches of species during the last glacial maximum compared to their present distribution. Increasing potential niche overlap among different species pairs possibly explains how lineages came into secondary contact, supporting the hypothesis of hybridization. In addition, morphological evolution is studied using geometric morphometrics on the network, and evidence of transgressive evolution has been found involving the pronotum shape, as well as highland/lowland habitat preferences. Finally, based on genomics and morphological data and using an integrative coalescent-based species delimitation approach, the separate evolution of two lineages in early stages of speciation is found. Taken together, dynamics of diversification of *Baripus* beetles in both space and time are discussed.

Introduction

Classically, the role of interspecific hybridization in animals has remained controversial (Mallet, 2005). With the advent of next-generation-sequencing technologies, empirical studies based on a huge number of different animal taxa continue to identify more cases in which interspecific hybridization has left insights along their genomes, even promoted speciation in many cases (reviewed in Taylor & Larson, 2019). In consequence, fresh, new perspectives that have been developed during the last decade have radically changed the view of the role of hybridization in species evolution, and it is now understood as an important mechanism for introducing new variants through which natural selection can work (Abbott et al., 2013, 2016; Gillespie et al., 2020; Marques et al., 2019; Taylor & Larson, 2019).

As a basic knowledge and a first requirement for understanding dynamics of diversification and speciation, the phylogenetic field has been challenged by the extensive impact of hybridization in species evolution. The multispecies coalescent (MSC) accommodates incomplete lineage sorting (ILS) as the only source of gene tree–species tree discordance, and it is blind to other possible sources. Thus, when interspecific gene flow is present, the MSC likely fails in recovering the true tree (Leaché et al., 2014; Long & Kubatko, 2018; Solís-Lemus et al., 2016). The newly proposed multispecies network coalescent model (MSNC; Blair & Ané, 2019; Degnan, 2018; Yu et al., 2012) can account both ILS and gene flow in phylogenetic network estimation. In addition, many possibilities of downstream analyses, such as testing transgressive evolution of phenotypes and reconstructing ancestral states, are now possible on networks (Blair & Ané, 2019; Teo et al., 2022). All these emerging methodological novelties are causing great excitement among researchers, given the tremendous potential for investigating the diversity of processes that are at work in young, rapidly diversifying and hybridizing lineages.

The Patagonian region of southern South America represents a geographically extensive and ecologically and topographically diverse area that remains biologically poorly

known. Andean uplift began in the Miocene and continues to the present, with repeated events of volcanic disturbances during the Pleistocene (Armijo et al., 2015; Ramos, 1989). Specifically, the Payunia biogeographic district, a ~450km linear extension (Cecilia Dominguez et al., 2006) in northern Patagonia in Neuquén-Mendoza provinces, contains more than 800 volcanoes reaching over 3000m that were formed between the Pliocene and Holocene (Ramos & Folguera, 2011). In addition, mountain building has been accompanied by multiple Pleistocene glaciations (Hollin & Schilling, 1981; Hulton et al., 2002; McCulloch & Bentley, 1998; Sugden et al., 2002; Wayne, 1995). This complex geoclimatic history in Patagonia drove repeated population contraction and expansion of different lineages, affecting not only the amount of intraspecific genetic diversity but also its spatial distribution and the connectivity among populations (Sérsic et al., 2011). Thus, studying environmental changes through time represents a valuable approach to understand dynamics of allopatric speciation and, possibly, secondary contact in biota from highland and lowland Patagonia. Specifically, climate variables can be accommodated in environmental niche models (ENM), and they might be useful to detect habitat fragmentation through time (maybe promoting speciation) or gain connectivity with others (as possible routes for migration and gene flow).

Baripus (*Cardiophthalmus*; Coleoptera: Carabidae, 20 species; Roig-Juñent et al., 2022) is one of the largest beetles endemic to Patagonia. It is distributed across grassland and shrub habitats, ranging from the lowlands in the very south of Patagonia, northern Tierra del Fuego, to isolated patches along the highland Andes and extra-Andes. Eight *Baripus* species are endemic to Payunia, including highland and lowland species ([Table 1](#)). Two species were never sampled in the same location (more than 2200 *Baripus* individuals stored in the IADIZA Entomological collection, Roig-Juñent et al., 2008), thus, they are considered strictly allopatric. Given the large body size of these beetles and the absence of wings, dispersal capabilities are likely limited. In addition, while linear distances between species distribution can be very small, differences in elevation likely act as barriers ([Fig. 1a](#)) as there are clear alterations in soil and vegetation. Furthermore, there are severe physiological challenges imposed to mountain insects, particularly those related to declined levels of oxygen, low temperature, and elevated levels of ultraviolet radiation (Bickler & Buck, 2007; Birrell et al., 2020; Blumthaler et al., 1997). However, *Baripus* species distributions have likely changed over time as dynamics in climate change probably forced species to move from the highlands to the lowlands during repeated glacial times (Agrain et al., 2021; Roig-Juñent et al., 2008, 2022). If refuge areas were shared between species when reproductive isolation was not yet complete, then secondary contact becomes a plausible hypothesis.

Here, dynamics of diversification of *Baripus* (*Cardiophthalmus*) species endemic to Payunia are studied using genomic RADseq data. Two candidate species are identified and hybridization between lowland and highland species is suggested in exploratory analyses. A phylogenetic network is reconstructed under MNSC (11 lineages). Based on environmental niche modeling, potential distributions of species are studied, both in the present and during the last glacial maximum (LGM, 21 kya). In addition, using geometric morphometrics, the morphological evolution on the network is performed, as well as a test for transgressive evolution of the pronotum shape. Finally, based on genomics and morphological data we find support for the early stages of separate evolution of two new species. Taken together, we discuss the dynamics of diversification of *Baripus* beetles in space and time.

Methods

Field sampling. Specimens were collected by hand or pitfall traps and stored in freezer with ethanol 96% at the Argentine Dryland Research Institute (IADIZA-CONICET) collection. Legs were separated for DNA extractions.

Library preparation and sequencing. High-molecular-weight genomic DNA was extracted for a total of 64 individuals representing all described species of the *Baripus* (*C.*) species complex from Payunia using the Qiagen DNeasy Blood & Tissue Kit (Qiagen, Valencia, USA) following the protocol provided by the manufacturer. Purified DNA was quantified using a Qubit 4.0 fluorimeter (Invitrogen, Carlsbad, USA). For each sample, 50 ng of DNA was used to construct double-digest restriction site-associated DNA (ddRAD) libraries using the quaddRAD protocol (Franchini et al., 2017) with a rare cutter, PstI, and a frequent cutter, MspI, restriction enzyme. Individually indexed samples (inner barcodes) were equimolarly pooled in six sub-pools. Each sub-pool was tagged with unique adapters and indexes (outer barcodes), its concentration and quality assessed with a Qubit 4.0 and a 2100 Bioanalyzer Instrument (Agilent, Palo Alto, USA), respectively, and finally pooled to form a single quaddRAD library including 64 individuals. The quaddRAD library was analyzed with a fragment analyzer and consequently size-selected from 450 to 650 bp in a Pippin Prep system (Sage Science, Beverly, USA) and paired-end sequenced (2x150 bp) in a HiSeq X-ten Illumina platform at the genome facility of BGI Genomics (BGI, Hong Kong).

Genomic data assembly. A total of 367 million (M) raw reads were processed by the clone_filter and process_radtags scripts implemented in the Stacks v2.54 package (Catchen et al., 2013) in order to remove PCR duplicates and demultiplex individuals while removing low-quality reads (process_radtags options: -c –q). Six individuals represented by <40,000 retained sequences were removed, thus, the final genomic dataset is composed of 58 individuals representing seven out of the eight described species (*B. nevado* was excluded due to low quality) plus two candidate species and two outgroups. A final data set of 364 M paired reads (averaging 6.3 M reads per individual) was used for downstream analysis. A *de novo* assembly was performed with dDocent (Puritz et al., 2014) using type of assembly = PE, clustering similarity 0.9 with minimum individual coverage 2 (k1 and k2), a mapping match value = 1 and mapping mismatch = 3, and gap penalty = 5. Complex

Table 1. Sampling.

Species	N_G	N_{GM}	Min. - Max. sampling altitude	Lowland/highland
B. mendozensis	8	44	1500–2300 m	Lowland
B. aff. mendozensis	4	4	1500 m	Lowland
B. precodillera	1	8	2800–3000 m	Highland
B. aucamahuida	5	18	1900–2200 m	Lowland
B. nevado	-	24	2300–3100 m	Highland
B. palauco	15	16	2600–3000 m	Highland
B. payun	3	22	2400–3050 m	Highland
B. gentilii	2	8	600–1500 m	Lowland
B. tromen	6	18	2100–2600 m	Highland
B. aff. tromen	4	6	2000–2800 m	Highland

Sampling sizes and classification of lowland/highland species. Abbreviations: N_G sampling size for genomics; N_{GM} sampling size for geometric morphometrics.

variants were processed using process_complex.py (Kautt et al., 2020). Indels were removed, and SNPs with a minimum depth 5 (−minDP) were filtered using vcftools v0.1.15 (Danecek et al., 2011). Missing data was filtered depending on the analysis (as specified below). Two other datasets were constructed using the full sequences (as required for some analyses, see below), one including 100 selected loci and a second one based on 300 loci (randomly selected among loci containing a number of substitutions within a 95% quantile of all observed loci). SNPs were phased using Beagle 5.4 (Browning et al., 2021), and long loci reconstructed based on the phased vcf file and reference sequences (from dDocent output).

Exploratory analyses. Individual ancestry components were estimated based on 24,304 SNPs (no missing data) representing all ingroup species (n = 50) using Admixture v1.3 (Alexander & Lange, 2011), including 5-fold cross-validation (−cv=5). Two additional admixture analyses were run only for two candidate species using 13,479 SNPs (*B. mendozensis* and *B. aff. mendozensis*, n = 12) and 16,567 SNPs (*B. tromen* and *B. aff. tromen*, n = 10). As this analysis showed possible admixed ancestry among different species, we statistically tested hybridization and estimated the inheritance parameter (γ) using the HyDe program (Blischak et al., 2018). HyDe uses phylogenetic invariants similar to the D-statistic (Patterson et al., 2012) to assess statistically significant evidence for hybridization. Specifically, we employed 7,430 SNPs (one random SNP per locus only, maximum missing data 0.2) considering 116 alleles (58 diploid individuals) in the python script run_hyde.py to test all triplet comparisons, including as hybrids *B. mendozensis, B. aff. mendozensis, B. precodillera, B. gentilii, B. tromen,* and *B. aff. tromen*.

Phylogenetic inference. A neighbor joining tree (NJ) and a coalescent-based phylogenetic tree were inferred using 7,430 SNPs (one random SNP per locus only, maximum missing data 0.2) and including a total 116 alleles (i.e., 58 individuals). Phylogenetic inferences were performed using the nj command and the coalescent-based program SVDquartets (Chifman & Kubatko, 2014) in PAUP* 4.0 (Swofford, 2003). The analysis was run by sampling one million random quartets and calculating 100 bootstrap replicates to assess statistical support. In SVDquartets, 11 lineages were considered, including seven described species, two candidate species, and two outgroups. A phylogenetic network under the multispecies network coalescent was inferred using PhyloNetworks program (Solís-Lemus et al., 2017). The program uses a pseudolikelihood approach and focuses on quartets, calculating the observed quartet concordance factor (CF). The CF of a given quartet (or split) is the proportion of trees supporting that particular quartet (Baum, 2007). A random SNP was extracted from each locus, and the input file of concordance factors for all possible 4-taxon combinations (330 species quartets in total) was generated using the SNPsCF function (www.github.com/melisaolave/SNPs2CF; Olave & Meyer, 2020). We sampled a total of 100 individual quartets (n.quartets = 100, between.species.only = TRUE) and used default values for all remaining settings. The phylogenetic networks were reconstructed using the function snaq! (Solís-Lemus & Ané, 2016) in PhyloNetworks (Solís-Lemus et al., 2017), including 20 independents runs with random seeds. We used the SVDquartet tree as starting topology and then inferred the networks using hmax = 0 (no hybridization), 1, 2, 3, and 4. Following the author's recommendations, we provided the hmax -1 network to the next inference. The best number of hybridization parameters was selected by plotting the likelihood scores and observing the tipping points in the distributions, i.e., a sharp improvement is expected until the number of hybridizing edges reaches the best value and a slower linear improvement thereafter. Bootstrap support was obtained from 50 pseudoreplicates using bootsnaq function and 10 runs per replicate. Finally, concordance factor histograms were plotted in order to investigate genome wide SNP discordance using the custom function plotCF (added to SNPs2CF since version 1.6). Histograms are used to illustrate deviation of CF, given that expectations of splits between closely related taxa are recovered with higher CFs, but the presence of a hybrid would be reflected in deviation of the two remaining CFs (Solís-Lemus & Ané, 2016).

Species niche models assessments. Environmental niche modeling (ENM) was employed to estimate species potential niches for hybridizing lineages as well as the candidate

species. Potential niches are niches where a species can live even though the species might not actually live there (compared to *realized* niche). Still, this estimation is useful to infer geographic areas that are or could have connected population/species, indicating possible routes available for migration or range shifts. Actual environmental information and species spatial occurrences as recorded in the entomological collection at IADIZA-CONICET were used to fit a model that explains the potential distribution of *Baripus* species in the present, as well as the environmental conditions during the last glacial maximum (LGM, 21kya). Climate layers at a resolution of 2.5 arc-min were obtained from the WorldClim 1.4 database (http://www.worldclim.org/), which comprises values for 19 bioclimatic (bc) variables, averaging the 1950–2000 period (Hijmans et al., 2005). Pearson's correlation analysis was performed on variables in order to avoid spatial correlation (Pearson >0.5) and reduce over-parametrization. As a result, five bioclimatic predictors were used: (bc1) mean annual temperature; (bc9) mean temperature of driest quarter; (bc12) annual precipitation; (bc15) precipitation seasonality; (bc18) precipitation of warmest quarter. The paleoclimate layers representing the LGM (21ky BP) were used to re-project to past species' spatial distribution. Paleoclimatic layers were also obtained from the WorldClim website, which includes downscaled climate data from different Global Climate Models (GCMs), based on original data made available by CMIP5 (Coupled Model Intercomparison Project Phase 5; http://cmip-pcmdi.llnl.gov/cmip5/); data were calibrated using WorldClim 1.4 as baseline of current climate. For the LGM we used three models: (i) CCSM4, Community Climate System Model (CCSM), National Center for Atmospheric Research; (ii) MPI-ESM, Max Planck Institute for Meteorology Earth System Model; and (iii) MIROC-ESM, Model for Interdisciplinary Research on Climate (MIROC), Japan Agency for Marine-Earth Science and Technology, Atmosphere and Ocean Research Institute, The University of Tokyo, and National Institute for Environmental Studies. Models were built using the maximum-entropy algorithm MaxEnt version 3.3.3k of the software (http://www.cs.princeton.edu/~schapire/maxent). To train models, we used 10,000 background points randomly extracted from the two-decimal degree buffers build on each species geographical localities (Feng et al., 2019). The potential distribution maps for each species were obtained from Maxent logistic output, which score habitat suitability with values ranging between 0 and 1 (where values close 0 indicate the worst suitability and values close to 1 indicate the best suitability). Other Maxent parameters were set to default values. The three LGM outputs based on different models were averaged and used for further analyses.

To test for significant ecological differences considering the habitat suitability scores, we performed niche identity tests using ENMTools 1.4.4 (www.enmtools.blogspot.com). A total of 99 replicates per species were performed. Finally, using the *I* statistic (Warren et al., 2008), we compared the degree of niche overlap between species pairs considering present and past species potential distributions.

Morphometric analyses. Body shape is an important trait that varies with habitat uses in Coleoptera (Forsythe, 1987). For geometric morphometric analyses a total of 202 photographs were included, corresponding to all species and candidate species included in genomic analysis + *B. nevado* (which had to be excluded from genomics due to low sequence quality). The configurations of points used in morphometric analyses of body shape (Fig. S1) were separated in two: pronotum and elytra. Pronotum shape comprised six fixed landmarks and 18 semi-landmarks. Elytra shape comprised four fixed landmarks and 14 semi-landmarks. Points were digitized on photographs using tpsDig v.2.32 (Rohlf, 2006). All further analyses were performed with the geomorph v3.0.6 R package (Adams & Otárola-Castillo, 2013). Landmarks were aligned using a full Procrustes superimposition with the function gpagen. Linear distances were obtained using the function interlmkdist, as follows: (i) for pronotum: length (LM4-13), width (LM9-17), apex width (LM 2-6), base width (12-14), anterior lateral margin width (right, LM8-19; left LM18-24), medium lateral margin width (right, LM9-20; left, LM17-23), posterior lateral margin width (right, LM10-21; left, LM16-22); (ii) for elytra: length (LM 1-8), maximum width (LM 5-11) and base width (14-2). Several exploratory analyses were performed. In all cases, allometry was controlled by regressing shape variables on body length and using regression residuals in subsequent analyses. Principal Component Analyses (PCA) were performed using the prcomp R function. Procrustes distances between groups of interest were performed using the procD.lm function. Consensus shapes were obtained using the mshape function, and plots of deviation were constructed with the plotRefToTarget function. A discriminant function was performed using the lda function of the MASS v7.3 library (Venables & Ripley, 2002).

Integrative species delimitation. We tested whether the two candidate species represent separate evolving lineages. We focused only on ingroup taxa (nine lineages), and we included a total of 100 alleles [50 diploid individuals] in 300 loci (long loci reconstructed as described in genomic assembly section), as well as a total of 34 morphological variables for 144 individuals, based on PC axes explaining up to 90% of shape variation (= first 11 PCs of pronotum shape and nine first PCs of elytra shape), plus pronotum and elytra length, their centroid sizes, and all remaining linear measurements (residuals after length correction) as described in *morphometric analyses* section. We used the program ibpp (Solís-Lemus et al., 2015), an extension of the popular program bpp (Z. Yang & Rannala, 2010) for species delimitation, which uses morphological and sequence data in an integrative framework. Similar to the original bpp, ibpp program begins with a guide tree and sequentially collapses internal nodes and calculates the posterior probability of each τ equal or different to 0. The search used a reversible MCMC (rjMCMC), with a prior specified from a gamma distribution as τ (branch length) and θ (= $N_e\mu$; where N_e is the population size and μ the mutation rate) for the molecular data, and a σ^2 (variance) and λ (within a between species ratio) for the morphological data. We included a prior distribution of θ and τ = G(1,1000), which

leads to a mean = 0.001, and left default values of σ^2 and κ = 0; thus, the priors are non-informative, and the program estimates them. We fine-tuned values during the analysis to ensure that they oscillate between 0.15 and 0.7 (as recommended in the program manual). We ran the MCMC analysis during 500,000 generations and sampled every 50,000 steps (10% burnin). As it has been shown that coalescent-based species delimitation models are sensitive to detect population structure (not species, Sukumaran & Knowles, 2017), we calculated the genealogical divergence index (*gdi*, Jackson et al., 2017) using the custom function get.gdi.R (available in www.github.com/melisaolave/mafalda). The *gdi* is calculated as $1-e^{-2\tau/\theta}$; where $-2\tau/\theta$ is the population divergence time in coalescent units, and $e^{-2\tau/\theta}$ is the probability that the two sequences within a population do not coalesce before reaching species divergence (τ) when we trace the genealogy backwards in time (Leaché et al., 2019). Even though deciding *what* is a species is necessarily subjective in current taxonomy (Sukumaran et al., 2021), using an integrative approach of morphological and genomic dataset in ibpp, plus applying *gdi a posteriori*, provides useful and more conservative information of the strength of divergence between pair of taxa (ranging from 0 [panmixia] to 1 [strong divergence]).

Trait evolution in a network. We investigated different phylogenetic comparative aspects of pronotum and elytra length and width evolution on the phylogenetic network using PhyloNetworks (Bastide et al., 2018; Teo et al., 2022). Given that network branch lengths need to be proportional to divergence times (instead of coalescent units), we estimated branch lengths for the backbone tree. Specifically, based on the estimated mitochondrial mutation rate for Carabidae = 0.0134 substitutions per site per million years (Pons et al., 2010), we approximated the nuclear substitution rate as four times smaller = 0.00335 substitutions per site per million year (i.e., mitochondria mutation rate is expected to be x4 greater than nuclear genes, Funk & Omland, 2003). This mutation rate matches well estimation for honeybees (S. Yang et al., 2015), as well as it is close to other insects (reviewed in Yoder & Tiley, 2021). A total of 100 loci (reconstructed as described in genomic assembly section) were used in starBEAST3 program (Douglas et al., 2022) under a Yule model, strict clocks per locus (unlinked), and JC69 substitution model per loci (unlinked). Species tree topology was fixed; a MCMC heuristic search was conducted during 50 million generations, sampling every 50,000 generations, and 10% burnin was applied. Convergence was assessed using Tracer v1.7.1 (Rambaut et al., 2018), relying in parameter estimation ESS > 200. Branch lengths were replaced in the phylogenetic network accordingly, and, using PhyloNetworks, we tested transgressive evolution (phylolm) for the pronotum length and width (continuous traits, allowing within species variation) and highland and lowland distributions (binary discrete trait, BTSM model). Transgressive evolution of phenotypes refers to traits that were inherited due to hybridization. In the case of highland-lowland distribution, it might indicate habitat preferences and possible loci associated with key

adaptations to habitat requirements. In PhyloNetworks, it is accommodated as a shifted Brownian motion model.

Results

Genomic analyses. The resulting NJ tree recovers the monophyly of all seven described species included in the genomic analyses (Fig. 1b). Individuals classified as *B. tromen* are recovered in two different clades, from now on called *B. tromen* and candidate species *B. aff. tromen*, consistent with ancestry estimation in an admixture analysis (CV: K1 = 1.17, K2 = 1.08). Similarly, one clade (*B. aff. mendozensis*) nested within *B. mendozensis* is recovered as a potential separate group in an admixture analysis (Fig. 1c, CV: K1 = 0.96, K2 = 1.02). Both candidate species present some proportion of mixed ancestry with their closely related lineage (Fig. 1c). Considering the full ingroup individuals (n = 50, seven described species plus two candidates), admixture returns the lowest CV in K5 = 0.26 (compared to K1 = 0.43, K2 = 0.35, K3 = 0.30, K4 = 0.28, K6 =0.28, and K7 = 0.28). Admixed ancestry is detected in *B. precordillera* (shared with *B. mendozensis* + *B. aff. mendozensis* and *B. palauco*) as well as *B. gentilii* ancestry shared with *B. payun*, *B. aucamahuida,* and *B. tromen*. A hybrid detection (HyDe) analysis is significant for several triplets involving *B. mendozensis* and *B. aff. mendozensis* as hybrids (Table 2).

A phylogenetic network analysis (Fig. 2a) recovers two hybridizing edges as the most likely network (net2: -P log lik = 54,038.86, compared to net0: -P log lik = 105,773.15, net1: -P log lik = 54,250.10). The backbone topology differs from a SVDquartet species tree based on MSC alone, particularly involving *B. gentilii* position (Fig. 2b). As an example, we show concordance factor histograms for some of quartets involving hybridizing lineages (*B. aff. mendozensis B. precordillera*, and *B. palauco* the ancestor of *B. mendozensis, B. aff. mendozensis, B. precordillera*) for which significant differences are detected among the three possible CF (Fig. 1c).

Environmental niche modeling results. Inference of potential niche for the target species involved in hybridization events show differences in latitudinal and altitudinal geographic location of potential niches between the present and the LGM in the four species (Fig. 3). *B. precordillera* potential niche distribution change from two allopatric patches (one between latitudes -33 and -34, and a second one between latitudes -36 and -38) to a continuum-like of potential niche distribution between latitude -32 to -38. Overlap of potential niche distribution increases significantly between the highland species *B. palauco* and the lowland *B. mendozensis*, as well as the highland species *B. palauco* and *B. precordillera* (Table 3). In addition, lineages involved in the second hybridizing edge, *B. precordillera* and *B. aff. mendozensis*, experienced a significant increase in potential niche overlap during the LGM (Table 3). Decrease of cell counts containing unique species, as well as an increase of cells counts containing three species, is observed in potential niches during the LGM compared to the present (Fig. 3).
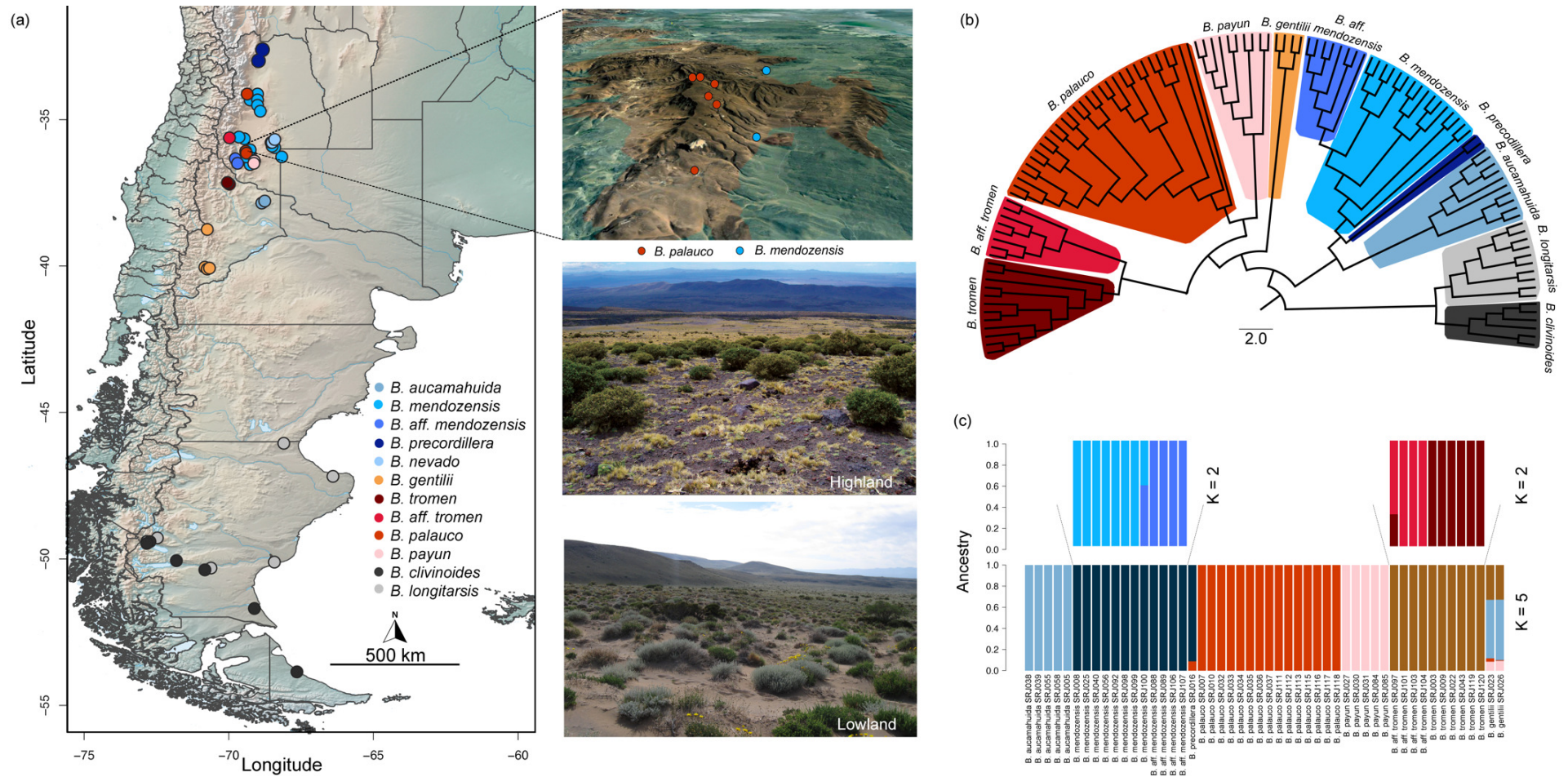
Figure 1. Sampling and exploratory analyses of genomic data.

(a) Sampling locations for individuals included in both genomics and geometric morphometric datasets. On the right, 3D representation of the distribution of a highland and a lowland species (*B. palauco* and *B. mendozensis*, respectively) and pictures of their environment (sandy vs. rocky). (b) Neighbor joining tree based on 7,430 SNPs for 116 alleles (diploid individuals). (c) Admixture plot constructed on 24,304 SNPs including all nine ingroup lineages (n = 50), as well as a separate analyses for the two candidate species, using 13,479 SNPs (*B. mendozensis* and *B. aff. mendozensis*, n = 12) and 16,567 SNPs (*B. tromen* and *B. aff. tromen*, n = 10).
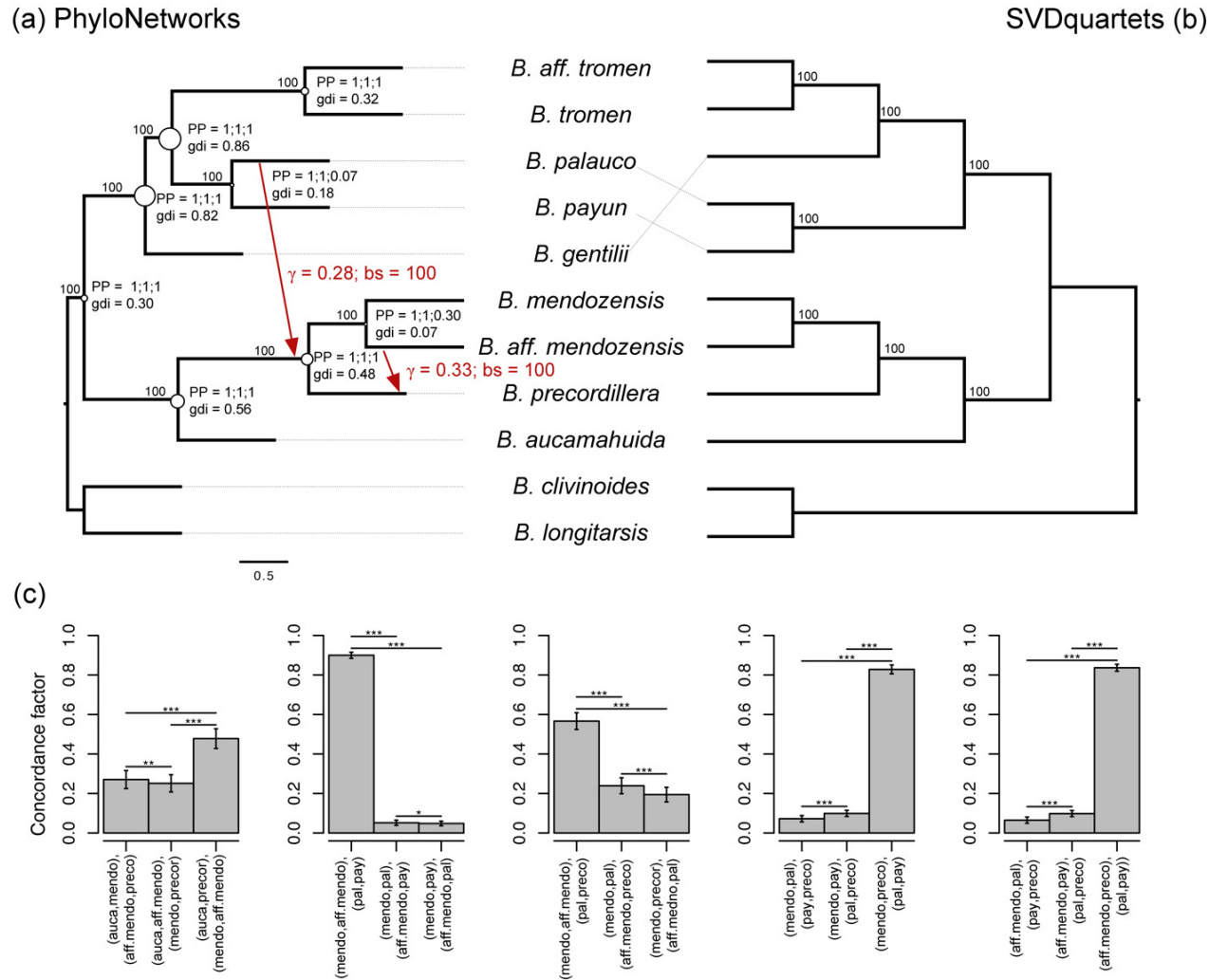
Figure 2. Phylogenetic reconstructions.

Phylogenetic results based on 7,430 SNPs and 116 alleles (diploid individuals) and using (a) PhyloNetworks and (b) SVDquartets. Bootstrap support (b.s.) are shown on nodes (all = 100). Circles sizes on nodes are proportional to *gdi* calculations (species delimitation analysis). Posterior probabilities (PP) of ibpp results are shown on each node, sorted as: combination of genomics + geometric morphometrics; genomics only; geometric morphometrics only. Arrows represent a hybridizing edge (or reticulation), and γ is the inheritance parameter. (c) Concordance factor calculations shown for five species quartets as examples. Vertical splits between closely related taxa are recovered with higher CFs, but the two remaining bars should be approximately equal in the absence of hybridization (i.e., horizontal inheritance would be reflected in deviation of the two remaining CFs). P values for significant differences (Student's t-test) are represented as <0.05*, <0.001**, and <0.0001***.

Table 2. Hybrid detection test.

P1	Hybrid	P2	Z score	P value	Gamma
B. tromen	*B. aff. mendozensis*	*B. precordillera*	6.02	8.80×10^{-10}	0.51
B. tromen	*B. mendozensis*	*B. precordillera*	5.84	2.56×10^{-9}	0.50
B. precordillera	*B. aff. mendozensis*	*B. aff. tromen*	5.21	9.58×10^{-8}	0.52
B. payun	*B. aff. mendozensis*	*B. precordillera*	5.15	1.31×10^{-7}	0.58
B. payun	*B. mendozensis*	*B. precordillera*	5.01	2.74×10^{-7}	0.57
B. precordillera	*B. mendozensis*	*B. aff. tromen*	4.99	3.09×10^{-7}	0.54
B. precordillera	*B. aff. mendozensis*	*B. palauco*	4.34	7.27×10^{-6}	0.40
B. precordillera	*B. mendozensis*	*B. palauco*	4.23	1.17×10^{-5}	0.40

Significant results (after Bonferroni correction) for hybrid detection (HyDe) test applied to all possible triplets including species detected with mixed ancestry in Fig. 1c.

Table 3. Environmental niche modeling.

Comparision		$I_{present}$	I_{LGM}	χ^2	df	p-value
	B. mendozensis	0.73	0.85	3.6468	1	0.02809*
B. palauco	*B. precordillera*	0.52	0.74	9.4595	1	0.00105**
	B. aff.mendozensis	0.54	0.45	1.2801	1	0.87110
B. precodillera	*B. aff. mendozensis*	0.17	0.29	3.7582	1	0.02627*
B. tromen	*B. aff. tromen*	0.80	0.76	0.2622	1	0.69570
B. mendozensis	*B. aff. mendozensis*	0.53	0.52	0.0001	1	0.50000

Statistical test for changes in proportion of geographic overlap in potential niches between the present and the LGM for selected lineages involved in hybridizing edges and the two candidate species.

Body shape differentiation. Large variation is found in linear measurements among species (Fig. S2). No significant differences are found in pairwise comparisons of the elytra shape (Table S1 and Fig. S4). Pronotum shape is significantly different among many species pairs (Table S1; Fig. 4), and highly significant differences in pronotum size are found between highland and lowland beetles (p << 0.001***; Table S2; Fig. S3). Among lineages involved in hybridization events*, B. palauco* pronotum shape is significantly different than *B. aff. mendozensis* and *B. precordillera* (p = 0.004** and p = 0.024*; respectively), and non-significant differences are detected between *B. palauco and B. mendozensis* (p = 0.17). *Baripus precordillera* has no significant differences in pronotum shape compared to both *B. mendozensis* and *B. aff. mendozensis*. Among candidate species, significant differences are found between *B. mendozensis* and *B. aff. mendozensis* (p = 0.012*) as well as between *B. tromen* and *B. aff. tromen* (p = 0.006**).

Trait evolution on the phylogenetic network. Transgressive evolution tests based on morphometrics return significant results for the pronotum width (Table 4, Table S5) for the hybridizing edge involving *B. palauco* and the ancestor of *B. precodillera + B. mendozensis + B. aff. mendozensis*. This result suggests that the pronotum width might have been inherited via gene flow as better fit than vertical inheritance. Pronotum length transgressive evolution is not significant (Table S4). In addition, testing the discrete lowland/highland transitions on the network return Bayes factor = 1.05, slightly greater than 1, could indicate that the habitat preference was inherited due to hybridization.

Species delimitation results. Either using genomic data alone or in combination with geometric morphometric data returns the fully split model as the most likely one (PP=1), including all nodes with PP = 1 (Fig. 2a). Using geometric morphometric data alone, it recovers the separate evolution of most lineages, including the candidate species *B. aff. tromen* (PP =1). However, using this dataset alone, there is reduced statistical support for the split between *B. mendozensis* and *B. aff. mendozensis* with PP = 0.30 as well as the split between *B. payun* and *B. palauco* with PP = 0.07. Measure of the strength of divergence (*gdi*) is reduced between *B. mendozensis* and *B. aff. mendozensis* (*gdi* = 0.07) as well as between formally described species *B. palauco* and *B. payun* (*gdi* = 0.18). Finally, *gdi* calculation for *B. tromen* and *B. aff. tromen* is = 0.32.

Discussion
Geographic shifts in highland and lowland species in response to climate change could have facilitated hybridization

Given its heterogeneity and complex geoclimatic history, the Andes mountains and nearby ranges offer an excellent opportunity to study lineage diversification in space and time. Here, integrative approach based on genomics, morphometrics, and environmental niche modeling are used to study the evolutionary dynamics of highland and lowland *Baripus* beetles. Exploratory genomic analyses reveal mixed ancestry of different species pairs (Fig. 1b), and a hybrid test detects highly significant hybrid ancestry of sev-
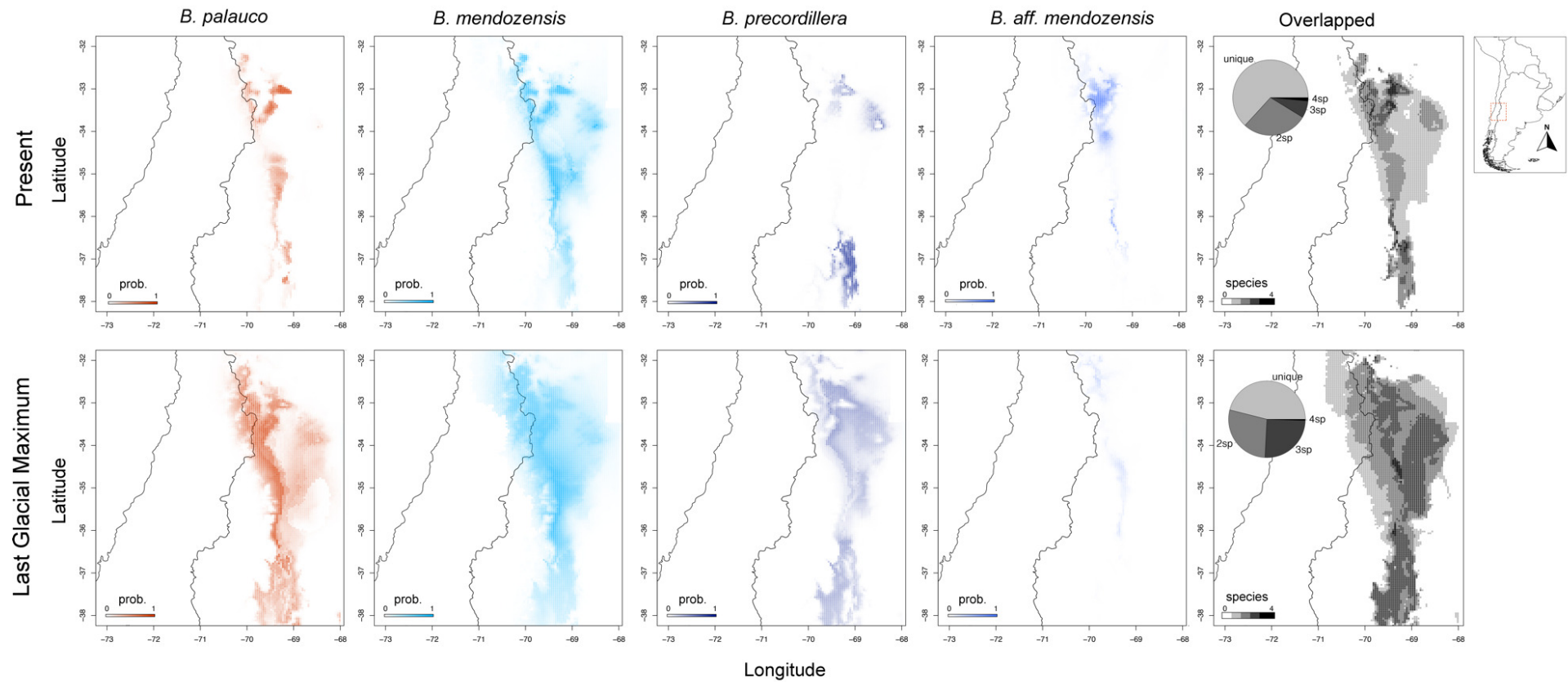
Figure 3. Environmental niche modeling.

Potential niche estimation during the present (above) and during the last glacial maximum (bottom). From left to right, predictions of potential niches for *B. palauco, B. mendozensis, B. precordillera,* and *B. aff. mendozensis*. Last panel on the right shows geographic overlap of potential niche distribution (after cut off > 0.1 prob.) of the four species. Pie charts represent the proportion of cell counts containing unique species occurrences and the overlap of two, three, or four species (in white-black scale).
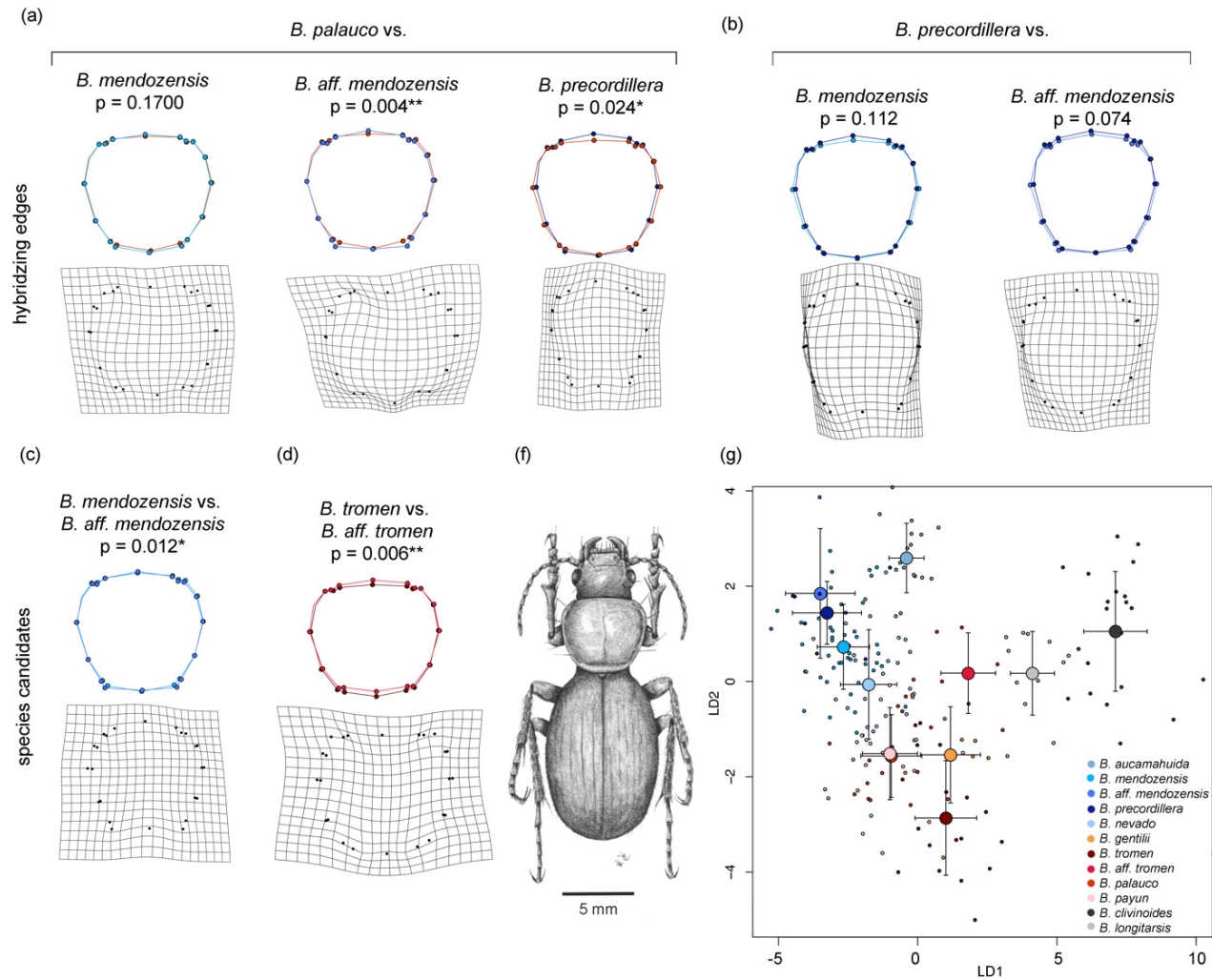
Figure 4. Pronotum shape variation.

Consensus shapes and deformation grids (magnified x3) are shown for pairwise comparisons, including (a) *B. palauco* vs. *B. mendozensis*, *B. aff. Mendozensis,* and *B. precordillera*; (b) *B. precordillera* vs. *B mendozensis* and *B. aff. mendozensis*; (c) *B. mendozensis* vs. *B. aff. mendozensis*; (d) *B. tromen* vs. *B. aff. tromen*. P-values for pairwise comparisons are shown in Table S1. (f) Scientific illustration of *B. mendozensis* as an example of body shape (credits to S. Roig-Juñent). (g) Discriminant analysis of pronotum shape.

Table 4. Trait evolution on a network.

Null Brownian motion model (no reticulations)						
Coef.	Std.	Error	t	Pr(>|t|)	Lower	95%
(Intercept)	6.09521	0.25383	24.01	$<1\times10^{-9}$	5.52964	6.66078
Phylogenetic variance rate = 0.3250; within species variance = 0.2010; Log likelihood = -123.5661; AIC = 253.1322						
Shifted Brownian motion model (with reticulations)						
Coef.	Std.	Error	t	Pr(>|t|)	Lower	95%
(Intercept)	6.1695	0.216639	28.48	<<0.001***	5.66993	6.66907
H1	-0.738596	0.289466	-2.55	0.0341*	-1.40611	-0.0710859
H2	-0.207666	0.337522	-0.62	0.5555	-0.985992	0.570661
Phylogenetic variance rate = 0.2242; within species variance = 0.1999; Log likelihood = -121.095; AIC = 252.189						

Phylogenetic regression result of transgressive evolution test for the pronotum width, considering the null tree-like Brownian motion model (above) and the network-like shifted Brownian model (bottom). H1 refers to the hybridizing edge involving *B. palauco* and the ancestor of *B. precodillera + B. mendozensis + B. aff. mendozensis;* H2 refers for the hybridizing edge involving *B. precordillera* and *B. aff. mendozensis*.

eral triplets (Table 2). A phylogenetic network recovers two hybridizing edges as the best explanation in *Baripus* beetle evolution. One hybridizing edge is inferred between the highland *B. precodillera* and the early divergent lineage of lowland *B. aff. mendozensis* (γ = 0.33). A second hybridization event (γ = 0.28) involves the highland adapted species *B. palauco* and the ancestor of a clade involving both lowland and highland lineages, *B. precodillera, B. mendozensis,* and *B. aff. mendozensis*. While geographic distribution of *B. palauco* is linearly close to *B. mendozensis*, allopatry of both species is pronounced due to elevation gradient (Fig. 1a). However, current species distributions probably changed through time as surviving *in situ* to drastic climatic changes is unlikely for the greatest extent of high-elevation biodiversity in Patagonia (Glasser et al., 2008). Instead, shifts in geographic distribution are expected for habitats offering more favorable conditions for survival. Interestingly, environmental niche modeling analyses have shown a significant increase of potential niche overlap during the LGM of *B. palauco* with *B. mendozensis* and *B. precordillera*, as well as between *B. precodillera* and *B. aff. mendozensis* (Fig. 3; Table 3). Here, the findings of potential shared refuge area occupied by *Baripus* beetles (Fig. 3) are consistent with other taxonomic groups in the so-called "valley refugia" (area surrounding latitude -36), including mice (Lessa et al. 2010) as well as a long list of co-distributed Patagonian plants (e.g., Jacob et al. 2009; Azipilicueta et al. 2009; Cosacov et al. 2010; Mathisasen and Premoli 2010; Premoli et al. 2010; reviewed in Sérsic et al., 2011).

Body shape in Coleoptera typically is modified according to habitat occupation (Forsythe, 1987). *Baripus* beetles are nocturnal, and, during daylight, they hide in holes built by themselves or under rocks (S.R.J. personal observation). Pronotum shape in beetles is important in order to reduce friction and cause less obstruction when burrowing or moving in confined spaces such as fissures in the ground (Forsythe, 1987). Here, lower elevations are represented by sandy soils, easier for excavation, while at higher elevations soil increases in granulometry and becomes rockier (Fig. 1a). Lowland and highland *Baripus* beetles have pronounced differences in pronotum size (Table S2). Inter-

estingly, transgressive evolution of pronotum width is detected (Table 4 and S4), a trait that might be involved in burrowing ability. This could be an important trait to allow *Baripus* to conquer higher elevation habitats. Highland/lowland habitat preferences is slightly supported as a transgressive trait, with Bayes factor = 1.05. Transgressive segregation may facilitate adaptation and invasion by hybrids into novel niches during ecological speciation (Abbott et al., 2013, 2016; Dittrich-Reed & Fitzpatrick, 2012; Gross & Rieseberg, 2005; Kagawa & Takimoto, 2018; Mallet, 2007; Pfennig et al., 2016; Rieseberg et al., 2007). Adaptive introgression has been reported in other groups of beetles (e.g., Huang, 2016; Lukicheva & Mardulyn, 2021), and, specifically, highland adapted species already carry complete set of genes which have already evolved under natural selection. Introgression of such genes to a newly arrived species can capitalize on adaptive solutions that have been refined over a much longer period of time in the donor species (Graham et al., 2021; Storz & Signore, 2021). Thus, our findings raise very interesting questions about the role of hybridization in allowing diversification into high elevation environments in *Baripus* species, which deserves further specific studies.

Early stages of differentiation of two separately evolving lineages in *Baripus* beetles

Genomic analyses have revealed individuals forming two separate clades, here called *B. aff. mendozensis* and *B. aff. tromen* (Fig. 1b-c). An admixture analysis returns a certain level of mixed ancestry as well as a paraphyletic inference of *B. mendozensis* in the neighbor joining tree (Fig. 1b-c). Moreover, *B. aff. mendozesis* is inferred to have recently hybridized with *B. precordillera* (Fig. 2a). An integrative species delimitation analysis under a model including genomics and morphometrics detects the separate evolution of these two candidate species (PP = 1), with reduced morphological divergence observed between *B. mendozensis* and *B. aff. mendozensis* (PP = 0.30). An analysis of the strength of divergence (*gdi*) demonstrates that both sepa-

rately evolving lineages are in early stages of differentiation (*gdi* = 0.07 and 0.32; Fig. 2a).

Based on genetic data alone, it has been proposed that *gdi* values ranging between 0.2 and 0.7 represent an ambiguous species limit, a gray zone of the speciation continuum, while values below 0.2 represent a single species (Jackson et al., 2017). Even though *gdi* provides valuable information about the strength of divergence, such cutting values are arbitrary for decision making in taxonomy. Besides genetics, other lines of evidence are always desired for a robust species delimitation (Edwards & Knowles, 2014; Olave et al., 2014; Sukumaran et al., 2021; Sukumaran & Knowles, 2017). Here, genetical and morphological differences in both candidate species have been shown (Fig. 1b, 2a, 4c-d, g), and specifically significant differences in pronotum shape are detected between *B. mendozensis* and *B. aff. mendozensis* (p = 0.0128*), as well as between *B. tromen* and *B. aff. tromen*. There are no significant changes in potential niche overlap through time with their sister lineages (Table 3), maybe indicating a stable, long-term geographic isolation (e.g., Dynesius & Jansson, 2014). Whether these two separately evolving lineages have accumulated enough differences in order to be classified as separate species deserves further taxonomic study.

Conclusions

Shifts in geographic distribution driven by historical climate change might have facilitated secondary contact between *Baripus* beetles. Moreover, we have found evidence of transgressive evolution of a potentially adaptive trait: the pronotum width. Finally, we found the existence of two separately evolving lineages in early stages of differentiation. *Baripus* beetles from the highlands in Patagonia represent an exciting system to study complex dynamics of diversification in heterogeneous and changing environments.

Data avilability

Genomic data has been uploaded to NCBI under accession PRJNA905331. All supporting files and data were uploaded to Dryad https://doi.org/10.5061/dryad.z34tmpgjv. SNPs2CF and plotCF functions are available in www.github.com/melisaolave/SNPs2CF, and custom described in Materials and Methods is available in www.github.com/melisaolave/mafalda

References

Abbott, R. J., Albach, D., Ansell, S., Arntzen, J. W., Baird, S. J. E., Bierne, N., Boughman, J., Brelsford, A., Buerkle, C. A., Buggs, R., Butlin, R. K., Dieckmann, U., Eroukhmanoff, F., Grill, A., Cahan, S. H., Hermansen, J. S., Hewitt, G., Hudson, A. G., Jiggins, C., … Zinner, D. (2013). Hybridization and speciation. *Journal of Evolutionary Biology*, *26*(2), 229–246. https://doi.org/10.1111/j.1420-9101.2012.02599.x

Abbott, R. J., Barton, N. H., & Good, J. M. (2016). Genomics of hybridization and its evolutionary consequences. *Molecular Ecology*, *25*(11), 2325–2332. https://doi.org/10.1111/mec.13685

Adams, D. C., & Otárola-Castillo, E. (2013). geomorph: an R package for the collection and analysis of geometric morphometric shape data. *Methods in Ecology and Evolution*, *4*(4), 393–399. https://doi.org/10.1111/2041-210x.12035

Agrain, F. A., Domínguez, C. M., Carrara, R., Griotti, M., & Roig-Juñent, S. A. (2021). Exploring the role of climatic niche changes in the evolution of the southern South American genus *Baripus* (Coleoptera: Carabidae): optimization of non-hereditary climatic variables and phylogenetic signal measurement. *Cladistics*, *37*(6), 816–828. https://doi.org/10.1111/cla.12464

Alexander, D. H., & Lange, K. (2011). Enhancements to the ADMIXTURE algorithm for individual ancestry estimation. *BMC Bioinformatics*, *12*(1). https://doi.org/10.1186/1471-2105-12-246

Armijo, R., Lacassin, R., Coudurier-Curveur, A., & Carrizo, D. (2015). Coupled tectonic evolution of Andean orogeny and global climate. *Earth-Science Reviews*, *143*, 1–35. https://doi.org/10.1016/j.earscirev.2015.01.005

Bastide, P., Solís-Lemus, C., Kriebel, R., William Sparks, K., & Ané, C. (2018). Phylogenetic comparative methods on phylogenetic networks with reticulations. *Systematic Biology*, *67*(5), 800–820. https://doi.org/10.1093/sysbio/syy033

Baum, D. A. (2007). Concordance trees, concordance factors, and the exploration of reticulate genealogy. *Taxon*, *56*(2), 417–426. https://doi.org/10.1002/tax.562013

Bickler, P. E., & Buck, L. T. (2007). Hypoxia tolerance in reptiles, amphibians, and fishes: life with variable oxygen availability. *Annual Review of Physiology*, *69*(1), 145–170. https://doi.org/10.1146/annurev.physiol.69.031905.162529

Birrell, J. H., Shah, A. A., Hotaling, S., Giersch, J. J., Williamson, C. E., Jacobsen, D., & Woods, H. A. (2020). Insects in high-elevation streams: Life in extreme environments imperiled by climate change. *Global Change Biology*, *26*(12), 6667–6684. https://doi.org/10.1111/gcb.15356

Blair, C., & Ané, C. (2019). Phylogenetic trees and networks can serve as powerful and complementary approaches for analysis of genomic data. *Systematic Biology*, *69*(3), 593–601. https://doi.org/10.1093/sysbio/syz056

Blischak, P. D., Chifman, J., Wolfe, A. D., & Kubatko, L. S. (2018). HyDe: a Python package for genome-scale hybridization detection. *Systematic Biology*, *67*(5), 821–829. https://doi.org/10.1093/sysbio/syy023

Blumthaler, M., Ambach, W., & Ellinger, R. (1997). Increase in solar UV radiation with altitude. *Journal of Photochemistry and Photobiology B: Biology*, *39*(2), 130–134. https://doi.org/10.1016/s1011-1344(96)00018-8

Browning, B. L., Tian, X., Zhou, Y., & Browning, S. R. (2021). Fast two-stage phasing of large-scale sequence data. *The American Journal of Human Genetics*, *108*(10), 1880–1890. https://doi.org/10.1016/j.ajhg.2021.08.005

Catchen, J., Hohenlohe, P. A., Bassham, S., Amores, A., & Cresko, W. A. (2013). Stacks: an analysis tool set for population genomics. *Molecular Ecology*, *22*(11), 3124–3140. https://doi.org/10.1111/mec.12354

Cecilia Dominguez, M., Roig-Junent, S., Tassin, J. J., Ocampo, F. C., & Flores, G. E. (2006). Areas of endemism of the Patagonian steppe: an approach based on insect distributional patterns using endemicity analysis. *Journal of Biogeography*, *33*(9), 1527–1537. https://doi.org/10.1111/j.1365-2699.2006.01550.x

Chifman, J., & Kubatko, L. (2014). Quartet inference from SNP data under the coalescent model. *Bioinformatics*, *30*(23), 3317–3324. https://doi.org/10.1093/bioinformatics/btu530

Danecek, P., Auton, A., Abecasis, G., Albers, C. A., Banks, E., DePristo, M. A., Handsaker, R. E., Lunter, G., Marth, G. T., Sherry, S. T., McVean, G., Durbin, R., & 1000 Genomes Project Analysis Group. (2011). The variant call format and VCFtools. *Bioinformatics*, *27*(15), 2156–2158. https://doi.org/10.1093/bioinformatics/btr330

Degnan, J. H. (2018). Modeling hybridization under the network multispecies coalescent. *Systematic Biology*, *67*(5), 786–799. https://doi.org/10.1093/sysbio/syy040

Dittrich-Reed, D. R., & Fitzpatrick, B. M. (2012). Transgressive hybrids as hopeful monsters. *Evolutionary Biology*, *40*(2), 310–315. https://doi.org/10.1007/s11692-012-9209-0

Douglas, J., Jiménez-Silva, C. L., & Bouckaert, R. (2022). StarBeast3: Adaptive Parallelized Bayesian Inference under the Multispecies Coalescent. *Systematic Biology*, *71*(4), 901–916. https://doi.org/10.1093/sysbio/syac010

Dynesius, M., & Jansson, R. (2014). Persistence of within-species lineages: a neglected control of speciation rates. *Evolution*, *68*(4), 923–934. https://doi.org/10.1111/evo.12316

Edwards, D. L., & Knowles, L. L. (2014). Species detection and individual assignment in species delimitation: can integrative data increase efficacy? *Proceedings of the Royal Society B: Biological Sciences*, *281*(1777), 20132765. https://doi.org/10.1098/rspb.2013.2765

Feng, X., Park, D. S., Liang, Y., Pandey, R., & Papeş, M. (2019). Collinearity in ecological niche modeling: Confusions and challenges. *Ecology and Evolution*, *9*(18), 10365–10376. https://doi.org/10.1002/ece3.5555

Forsythe, T. G. (1987). The relationship between body form and habit in some Carabidae (Coleoptera). *Journal of Zoology*, *211*(4), 643–666. https://doi.org/10.1111/j.1469-7998.1987.tb04477.x

Franchini, P., Monné Parera, D., Kautt, A. F., & Meyer, A. (2017). quaddRAD: a new high-multiplexing and PCR duplicate removal ddRAD protocol produces novel evolutionary insights in a nonradiating cichlid lineage. *Molecular Ecology*, *26*(10), 2783–2795. https://doi.org/10.1111/mec.14077

Funk, D. J., & Omland, K. E. (2003). Species-level paraphyly and polyphyly: frequency, causes, and consequences, with insights from animal mitochondrial DNA. *Annual Review of Ecology, Evolution, and Systematics*, *34*(1), 397–423. https://doi.org/10.1146/annurev.ecolsys.34.011802.132421

Gillespie, R. G., Bennett, G. M., De Meester, L., Feder, J. L., Fleischer, R. C., Harmon, L. J., Hendry, A. P., Knope, M. L., Mallet, J., Martin, C., Parent, C. E., Patton, A. H., Pfennig, K. S., Rubinoff, D., Schluter, D., Seehausen, O., Shaw, K. L., Stacy, E., Stervander, M., ... Wogan, G. O. U. (2020). Comparing adaptive radiations across space, time, and taxa. *Journal of Heredity*, *111*(1), 1–20. https://doi.org/10.1093/jhered/esz064

Glasser, N. F., Jansson, K. N., Harrison, S., & Kleman, J. (2008). The glacial geomorphology and Pleistocene history of South America between 38°S and 56°S. *Quaternary Science Reviews*, *27*(3–4), 365–390. https://doi.org/10.1016/j.quascirev.2007.11.011

Graham, A. M., Peters, J. L., Wilson, R. E., Muñoz-Fuentes, V., Green, A. J., Dorfsman, D. A., Valqui, T. H., Winker, K., & McCracken, K. G. (2021). Adaptive introgression of the beta-globin cluster in two Andean waterfowl. *Heredity*, *127*(1), 107–123. https://doi.org/10.1038/s41437-021-00437-6

Gross, B. L., & Rieseberg, L. H. (2005). The ecological genetics of homoploid hybrid speciation. *Journal of Heredity*, *96*(3), 241–252. https://doi.org/10.1093/jhered/esi026

Hijmans, R. J., Cameron, S. E., Parra, J. L., Jones, P. G., & Jarvis, A. (2005). Very high resolution interpolated climate surfaces for global land areas. *International Journal of Climatology*, *25*(15), 1965–1978. https://doi.org/10.1002/joc.1276

Hollin, J., & Schilling, D. (1981). Late Wisconsin-Weichselian mountain glaciers and small ice caps. In G. H. Denton & T. J. Hughes (Eds.), *The Last Great Ice Sheets* (pp. 179–206).

Huang, J.-P. (2016). Parapatric genetic introgression and phenotypic assimilation: testing conditions for introgression between Hercules beetles (*Dynastes*, Dynastinae). *Molecular Ecology*, *25*(21), 5513–5526. https://doi.org/10.1111/mec.13849

Hulton, N. R. J., Purves, R. S., McCulloch, R. D., Sugden, D. E., & Bentley, M. J. (2002). The last glacial maximum and deglaciation in southern South America. *Quaternary Science Reviews*, *21*(1–3), 233–241. https://doi.org/10.1016/s0277-3791(01)00103-2

Jackson, N. D., Carstens, B. C., Morales, A. E., & O.'Meara. (2017). Species delimitation with gene flow. *Syst Biol*, *66*, 799–812.

Kagawa, K., & Takimoto, G. (2018). Hybridization can promote adaptive radiation by means of transgressive segregation. *Ecology Letters*, *21*(2), 264–274. https://doi.org/10.1111/ele.12891

Kautt, A. F., Kratochwil, C. F., Nater, A., Machado-Schiaffino, G., Olave, M., Henning, F., Torres-Dowdall, J., Härer, A., Hulsey, C. D., Franchini, P., Pippel, M., Myers, E. W., & Meyer, A. (2020). Contrasting signatures of genomic divergence during sympatric speciation. *Nature*, *588*(7836), 106–111. https://doi.org/10.1038/s41586-020-2845-0

Leaché, A. D., Harris, R. B., Rannala, B., & Yang, Z. (2014). The influence of gene flow on species tree estimation: a simulation study. *Systematic Biology*, *63*(1), 17–30. https://doi.org/10.1093/sysbio/syt049

Leaché, A. D., Zhu, T., Rannala, B., & Yang, Z. (2019). The spectre of too many species. *Systematic Biology*, *68*(1), 168–181. https://doi.org/10.1093/sysbio/syy051

Long, C., & Kubatko, L. (2018). The effect of gene flow on coalescent-based species-tree inference. *Systematic Biology*, *67*(5), 770–785. https://doi.org/10.1093/sysbio/syy020

Lukicheva, S., & Mardulyn, P. (2021). Whole-genome sequencing reveals asymmetric introgression between two sister species of cold-resistant leaf beetles. *Molecular Ecology*, *30*(16), 4077–4089. https://doi.org/10.1111/mec.16011

Mallet, J. (2005). Hybridization as an invasion of the genome. *Trends in Ecology & Evolution*, *20*(5), 229–237. https://doi.org/10.1016/j.tree.2005.02.010

Mallet, J. (2007). Hybrid speciation. *Nature*, *446*(7133), 279–283. https://doi.org/10.1038/nature05706

Marques, D. A., Meier, J. I., & Seehausen, O. (2019). A combinatorial view on speciation and adaptive radiation. *Trends in Ecology & Evolution*, *34*(6), 531–544. https://doi.org/10.1016/j.tree.2019.02.008

McCulloch, R. D., & Bentley, M. J. (1998). Late glacial ice advances in the Strait of Magellan, southern Chile. *Quaternary Science Reviews*, *17*(8), 775–787. https://doi.org/10.1016/s0277-3791(97)00074-7

Olave, M., & Meyer, A. (2020). Implementing Large Genomic Single Nucleotide Polymorphism Data Sets in Phylogenetic Network Reconstructions: A Case Study of Particularly Rapid Radiations of Cichlid Fish. *Systematic Biology*, *69*(5), 848–862. https://doi.org/10.1093/sysbio/syaa005

Olave, M., Solà, E., & Knowles, L. L. (2014). Upstream analyses create problems with DNA-based species delimitation. *Systematic Biology*, *63*(2), 263–271. https://doi.org/10.1093/sysbio/syt106

Patterson, N., Moorjani, P., Luo, Y., Mallick, S., Rohland, N., Zhan, Y., Genschoreck, T., Webster, T., & Reich, D. (2012). Ancient admixture in human history. *Genetics*, *192*(3), 1065–1093. https://doi.org/10.1534/genetics.112.145037

Pfennig, K. S., Kelly, A. L., & Pierce, A. A. (2016). Hybridization as a facilitator of species range expansion. *Proceedings of the Royal Society B: Biological Sciences*, *283*(1839), 20161329. https://doi.org/10.1098/rspb.2016.1329

Pons, J., Ribera, I., Bertranpetit, J., & Balke, M. (2010). Nucleotide substitution rates for the full set of mitochondrial protein-coding genes in Coleoptera. *Molecular Phylogenetics and Evolution*, *56*(2), 796–807. https://doi.org/10.1016/j.ympev.2010.02.007

Puritz, J. B., Hollenbeck, C. M., & Gold, J. R. (2014). *dDocent*: a RADseq, variant-calling pipeline designed for population genomics of non-model organisms. *PeerJ*, *2*(4), e431. https://doi.org/10.7717/peerj.431

Rambaut, A., Drummond, A. J., Xie, D., Baele, G., & Suchard, M. A. (2018). Posterior summarization in Bayesian phylogenetics using Tracer 1.7. *Systematic Biology*, *67*(5), 901–904. https://doi.org/10.1093/sysbio/syy032

Ramos, V. A. (1989). Andean foothills structures in northern Magallanes Basin, Argentina. *AAPG Bulletin*, *73*, 887–903. https://doi.org/10.1306/44b4a28a-170a-11d7-8645000102c1865d

Ramos, V. A., & Folguera, A. (2011). Payenia volcanic province in the Southern Andes: An appraisal of an exceptional Quaternary tectonic setting. *Journal of Volcanology and Geothermal Research*, *201*(1–4), 53–64. https://doi.org/10.1016/j.jvolgeores.2010.09.008

Rieseberg, L. H., Kim, S.-C., Randell, R. A., Whitney, K. D., Gross, B. L., Lexer, C., & Clay, K. (2007). Hybridization and the colonization of novel habitats by annual sunflowers. *Genetica*, *129*(2), 149–165. https://doi.org/10.1007/s10709-006-9011-y

Rohlf, F. J. (2006). *tpsDig, version 2.10*. http://life.bio.sunysb.edu/morph/index.html

Roig-Juñent, S. A., Agrain, F., Carrara, R., Ruiz-Manzanos, E., & Tognelli, M. F. (2008). Description and phylogenetic relationships of two new species of Baripus (Coleoptera: Carabidae: Broscini) and considerations regarding patterns of speciation. *Annals of Carnegie Museum*, *77*(1), 211–227. https://doi.org/10.2992/0097-4463-77.1.211

Roig-Juñent, S. A., Cisterna, G., Griotti, M., & Austin, A. (2022). Phylogeny of the South American genus Baripus (Coleoptera: Carabidae: Broscini) with the description of new mountain species from the northern Patagonia Biogeographic Province. *Invertebrate Systematics*, *36*(3), 226–243. https://doi.org/10.1071/is21028

Sérsic, A. N., Cosacov, A., Cocucci, A. A., Johnson, L. A., Pozner, R., Avila, L. J., Sites, J. W., Jr., & Morando, M. (2011). Emerging phylogeographical patterns of plants and terrestrial vertebrates from Patagonia. *Biological Journal of the Linnean Society*, *103*(2), 475–494. https://doi.org/10.1111/j.1095-8312.2011.01656.x

Solís-Lemus, C., & Ané, C. (2016). Inferring phylogenetic networks with maximum pseudolikelihood under incomplete lineage sorting. *PLos Genetics*, *12*(3), e1005896. https://doi.org/10.1371/journal.pgen.1005896

Solís-Lemus, C., Bastide, P., & Ané, C. (2017). PhyloNetworks: a package for phylogenetic networks. *Molecular Biology and Evolution*, *34*(12), 3292–3298. https://doi.org/10.1093/molbev/msx235

Solís-Lemus, C., Knowles, L. L., & Ané, C. (2015). Bayesian species delimitation combining multiple genes and traits in a unified framework. *Evolution*, *69*(2), 492–507. https://doi.org/10.1111/evo.12582

Solís-Lemus, C., Yang, M., & Ané, C. (2016). Inconsistency of species tree methods under gene flow. *Systematic Biology*, *65*(5), 843–851. https://doi.org/10.1093/sysbio/syw030

Storz, J. F., & Signore, A. V. (2021). Introgressive hybridization and hypoxia adaptation in high-altitude vertebrates. *Frontiers in Genetics*, *12*(696484). https://doi.org/10.3389/fgene.2021.696484

Sugden, D. E., Hulton, N. R. J., & Purves, R. S. (2002). Modelling the inception of the Patagonian icesheet. *Quaternary International*, *95–96*, 55–64. https://doi.org/10.1016/s1040-6182(02)00027-7

Sukumaran, J., Holder, M. T., & Knowles, L. L. (2021). Incorporating the speciation process into species delimitation. *PLOS Computational Biology, 17*(5), e1008924. https://doi.org/10.1371/journal.pcbi.1008924

Sukumaran, J., & Knowles, L. L. (2017). Multispecies coalescent delimits structure, not species. *Proceedings of the National Academy of Sciences*, *114*(7), 1607–1612. https://doi.org/10.1073/pnas.1607921114

Swofford, L. (2003). *PAUP*: Phylogenetic Analysis Using Parsimony (*and Other Methods)*. Sinauer Associates.

Taylor, S. A., & Larson, E. L. (2019). Insights from genomes into the evolutionary importance and prevalence of hybridization in nature. *Nature Ecology & Evolution*, *3*(2), 170–177. https://doi.org/10.1038/s41559-018-0777-y

Teo, B., Rose, J. P., Bastide, P., & Ané, C. (2022). Accounting for within-species variation in continuous trait evolution on a phylogenetic network. *bioRxiv*. https://doi.org/10.1101/2022.05.12.490814

Venables, W. N., & Ripley, B. D. (2002). *Modern Applied Statistics with S*. Springer New York. https://doi.org/10.1007/978-0-387-21706-2

Warren, D. L., Glor, R. E., & Turelli, M. (2008). Environmental niche equivalency versus conservatism: quantitative approaches to niche evolution. *Evolution*, *62*(11), 2868–2883. https://doi.org/10.1111/j.1558-5646.2008.00482.x

Wayne, W. J. (1995). Quaternary Geology and Geomorphology of South America. *Geomorphology*, *11*(4), 347–349. https://doi.org/10.1016/0169-555x(95)90014-k

Yang, S., Wang, L., Huang, J., Zhang, X., Yuan, Y., Chen, J.-Q., Hurst, L. D., & Tian, D. (2015). Parent–progeny sequencing indicates higher mutation rates in heterozygotes. *Nature*, *523*(7561), 463–467. https://doi.org/10.1038/nature14649

Yang, Z., & Rannala, B. (2010). Bayesian species delimitation using multilocus sequence data. *Proceedings of the National Academy of Sciences*, *107*(20), 9264–9269. https://doi.org/10.1073/pnas.0913022107

Yoder, A. D., & Tiley, G. P. (2021). The challenge and promise of estimating the de novo mutation rate from whole-genome comparisons among closely related individuals. *Molecular Ecology*, *30*(23), 6087–6100. https://doi.org/10.1111/mec.16007

Yu, Y., Degnan, J. H., & Nakhleh, L. (2012). The probability of a gene tree topology within a phylogenetic network with applications to hybridization detection. *PLoS Genetics*, *8*(4), e1002660. https://doi.org/10.1371/journal.pgen.1002660